ELSEVIER

Journal of Atmospheric and Solar-Terrestrial Physics 70 (2008) 836–853

Journal of ATMOSPHERIC AND SOLAR-TERRESTRIAL PHYSICS

www.elsevier.com/locate/jastp

Ionospheric behavior over Europe during the solar eclipse of 3 October 2005

N. Jakowski[a,*], S.M. Stankov[a], V. Wilken[a], C. Borries[a], D. Altadill[b], J. Chum[c], D. Buresova[c], J. Boska[c], P. Sauli[c], F. Hruska[c], Lj.R. Cander[d]

[a]*DLR Institute of Communications and Navigation, Kalkhorstweg 53, D-17235 Neustrelitz, Germany*
[b]*Observatorio del Ebro, Universitat Ramon Llull, Crta. de l'Observatori No. 8, E-43520 Roquetes, Spain*
[c]*Institute of Atmospheric Physics, Bocni II/1401, 14131 Praha 4, Czech Republic*
[d]*Rutherford Appleton Laboratory, Chilton OX11 0QX, UK*

Accepted 20 February 2007
Available online 26 January 2008

Abstract

An annular eclipse occurred over Europe in the morning hours of 3 October 2005. The well-defined obscuration function of the solar radiation during the eclipse provided a good opportunity to study the ionospheric/thermospheric response to solar radiation changes. Since the peak electron density behavior of the ionospheric F2 layer follows the local balance of plasma production, loss and transport, the ionospheric plasma redistribution processes significantly affect the shape of the electron density profile. These processes are discussed here based on a comparison of vertical incidence sounding (VS) and vertical total electron content (TEC) data above-selected ionosonde stations in Europe. The equivalent slab thickness, derived with a time resolution of 10 min, provides relatively good information on the variation of the electron density profile during the eclipse. The computations reveal an increased width of the ionosphere around the maximum phase. As indicated by the available measurements over Spain, the photo production is significantly reduced during the event leading to a slower increase of the total ionization in comparison with the neighboring days. The supersonic motion of the Moon's cool shadow through the atmosphere may generate atmospheric gravity waves that propagate upward and are detectable as traveling ionospheric disturbances at ionospheric heights. High-frequency (HF) Doppler shift spectrograms were recorded during the eclipse showing a distinct disturbance along the eclipse path. Whereas the ionosonde measurements at the Ebro station/Spain in the vicinity of the eclipse path reveal the origin of the wave activity in the lower thermosphere below about 180 km altitude, the similar observations at Pruhonice/Czech Republic provide arguments to localize the origin of the abnormal waves in the middle atmosphere well below the ionospheric heights. Although ionosonde and HF Doppler measurements show enhanced wave activity, the TEC data analysis does not, which is an indication that the wave amplitudes are too small for detecting them via this interpolation method. The total ionization reduces up to about 30% during the event. A comparison with similar observations from the solar eclipse of 11 August 1999 revealed a quite different ionospheric behavior at different latitudes, a fact that needs further investigation.

Keywords: Ionosphere; Solar eclipse; Vertical sounding; GPS sounding; Gravity waves

*Corresponding author.
E-mail address: norbert.jakowski@dlr.de (N. Jakowski).

1364-6826/$ - see front matter © 2008 Elsevier Ltd. All rights reserved.
doi:10.1016/j.jastp.2007.02.016

1. Introduction

An annular solar eclipse occurred on 3 October 2005, first observed over the North Atlantic at 08:41 UT, reaching the northern coast of Spain and Portugal at 08:51 UT, continuing over Africa and last observed over the Indian Ocean (Fig. 1). It was a rare event allowing a new, better equipped investigation of the ionospheric response to solar eclipses by using several European observation facilities (Altadill et al., 2001; Jakowski et al., 2001). To get a comprehensive view on the eclipse by utilizing different observation techniques, the European COST Action 296 (http://www.cost296.rl.ac.uk/) has initiated a specific measuring campaign whose preliminary results are reported here.

The obscuration function of the solar radiation during a solar eclipse is very helpful for studying the induced spatial and temporal ionosphere/thermosphere variations. The attenuation of the solar EUV irradiation and the thermospheric heating lead to a number of closely related phenomena in the ionosphere. The ionospheric response to solar eclipses has been the purpose of many works, both theoretical and experimental. Changes in the ionospheric plasma density and temperature, diffusion processes, etc., have already been studied and time constants estimated (Baron and Hunsuker, 1973; Jakowski et al., 1983; Cohen, 1984; Mueller-Wodarg et al., 1998; Huang et al., 1999; McPherson et al., 2000; and the references therein). Thus, it is now proven that the plasma redistribution during eclipses may lead to modifications of the electron density profile shape, measurable by the equivalent slab thickness. The latter can be derived from simultaneous vertical incidence sounding (VS) and total electron content (TEC) measurements carried out over a given ionosonde station (Fig. 2). Principally, it is expected that the relative depletion of ionization is more significant in the bottom-side ionosphere, at around 200 km altitude, where the photo ionization is maximum and the recombination is strong. If ignoring dynamic forces such as meridional thermospheric winds and electric fields, enhancement of both the peak electron density height (h_mF2) and the slab thickness (τ) should be observed. However, the existence of horizontal winds or vertical redistribution induced by electric fields may lead to other effects. Since the geomagnetic conditions before and during the eclipse on 3 October 2005 did not indicate strong perturbations of magnetospheric origin, it is reasonable to expect that diffusive transport processes dominated during this event. If so, we should observe a delayed response to the obscuration function and the delay should increase with height.

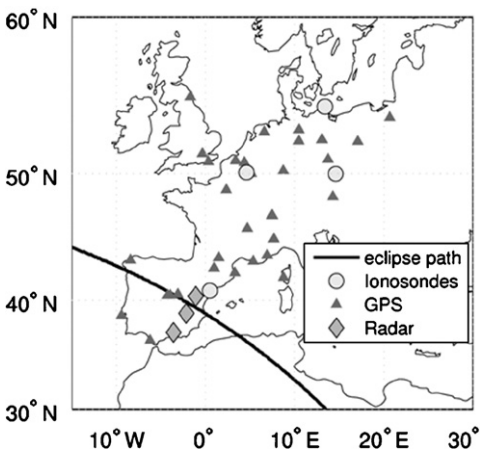

Fig. 1. Geographical distribution of the European GPS receivers, ionosonde, and radar observation stations. The black line indicates the path of the eclipse shadow of the obscuration at ground level. The circles mark the location of ionosonde stations, the triangles show the location of GPS receivers and the diamonds indicate the locations of the HF Doppler radar sites.

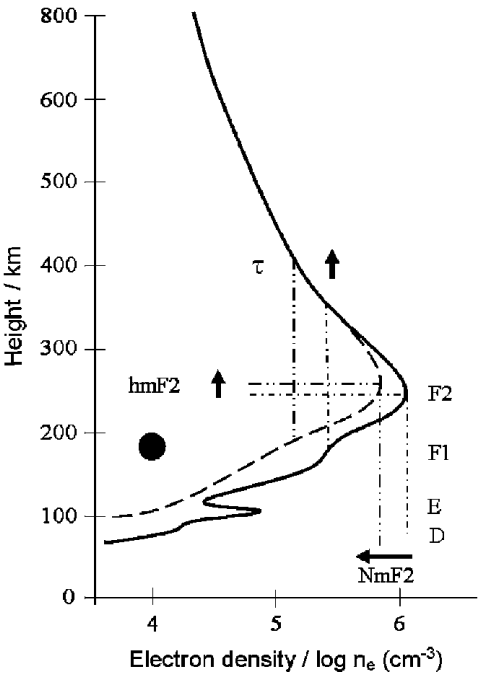

Fig. 2. Sketch of plasma redistribution processes mainly in the bottom-side ionosphere indicated by changes in the key parameters: peak density N_mF2, peak height h_mF2, slab thickness τ.

Due to the supersonic speed of the Moon's cool shadow in the atmosphere, atmospheric gravity waves (AGW) may be generated as theoretically predicted by Chimonas and Hines (1970). Such waves propagate upward with growing amplitudes and their ionospheric trace should be measurable as traveling ionosphere disturbances (TIDs). Evidences of AGW occurrence in the ionosphere after the solar eclipse of 23 September 1987 was for example given by Cheng et al. (1992) while Fritts and Luo (1993) modeled the gravity wave field induced by the cooling of the ozone layer in response to the solar eclipse on 11 July 1991. They explained the observations with the generation of upward propagating waves with dominant periods between 2 and 4 h. Liu et al. (1998) found internal gravity waves vertically propagating from the F1 layer in the ionosphere during the solar eclipse of 24 October 1995. Farges et al. (2003) analyzed results of the atmospheric pressure carried out using microbarographs located on the ground level and results of ionospheric sounding using the Francourville (FRC) array during the solar eclipse of 11 August 1999. They proposed two sources of AGW: a source located in the lower atmosphere, observed in the microbarograph records, and a source located in the thermosphere, as detected in VS ionograms. The wave observed via the electron density fluctuations showed a characteristic period of approximately 60 min. Detected changes in ionization attained 55% during the total eclipse with respect to the reference day of 12 August 1999. Sauli et al. (2006a) reported occurrences of acoustic gravity waves excited at ionospheric F-layer height during the solar eclipse of 11 August 1999. During the initial phase, they found acoustic and gravity waves generated in the region around 200 km propagating upward and downward simultaneously. During the recovery phase, they detected waves propagating from below, from the atmospheric regions. A similar effect was found by Altadill et al. (2001). The analysis must take into account the possibility of other sources capable of generating AGW, such as the meteorological weather front or the solar terminator (Jakowski et al., 2001).

The aim of this paper is to present a preliminary analysis of the 3 October 2005 eclipse effects on the ionosphere over Europe based on VS and GPS measurements. The VS measurements provide electron density profiles with high vertical resolution but with rather scarce spatial resolution. However, the dense network of GPS stations provides higher spatial resolution of integral TEC data. Some of the eclipse effects on the vertical ionospheric structure have been analyzed from VS or GPS records alone, effects on the regional structure of the ionosphere have been analyzed from GPS records, and the slab thickness has been obtained from combining VS and GPS measurements. In addition, some of the ionospheric effects are compared with similar effects observed during the total eclipse on 11 August 1999.

2. Database

2.1. Vertical incidence sounding data

The VS measurements provide information on the local electron density distribution of the bottomside ionosphere. The following sounding stations contributed to this study: Ebro/Spain (40.8°N, 0.5°E), Pruhonice/Czech Republic (49.9°N, 14.5°E), Dourbes/Belgium (50.1°N, 4.6°E), and Juliusruh/Germany (54.6°N, 13.4°E).

The Ebro observatory performed a measurement campaign at a 5 min sampling rate from 1 to 5 October 2005 using the digital sounder DGS-256 (http://ulcar.uml.edu/). The ionograms have been manually checked with the Digisonde Ionogram Data Visualization/Editing Tool (SAO-X) in order to avoid possible mistakes of the Automatic Real Time Ionogram Scaler with True Height (ARTIST) (Huang and Reinisch, 1996; Reinisch et al., 2005; and the references therein). Following that, 'true' height electron density profiles have been computed with the True Height Profile Inversion Tool (NHPC 4.30) included in SAO-X. The solar eclipse over Ebro started at 07:42 UT (at ground level) and ended at 10:29 UT with the maximum obscuration of the Moon occurring at 09:02 UT. Each plasma frequency profile has been considered as a function of time and height. Notice that the plasma frequency, f_p, relates to the electron density, $N(h)$, at a given altitude h in the following manner: $N(h) = 1.24 \times 10^{-2} f_p^2(h)$, where the electron density and the plasma frequency are given in SI units. The profiles have been obtained from the base of the E layer up to 450 km. Nevertheless, we restricted our study to the altitude range between the base of the F-region and the peak electron density height, h_mF2. This is done in order to avoid the strong modeling effects caused by the algorithm on the E–F valley region and on the topside. Therefore, the height range under analysis is 140–230 km during daytime and 250–350 km during nighttime. The profiles were

calculated with an altitude step of 5 km and, consequently, two types of time series were obtained—the plasma frequency at fixed heights and the reflection altitude at fixed frequencies. The time series of plasma frequency at fixed altitudes enables the study of the electron density variations as a function of time and altitude and the time series of the altitude at fixed frequencies allow the investigation of the ionospheric dynamics.

At the Pruhonice observatory, the electron density profile was measured every 2 min using a DPS-4 sounder. The high-rate sampling campaign started at 6.36 UT and finished at 15.58 UT, thus covering the entire eclipse event. Such a high sampling rate allows us to make precise parameterization of the electron density fluctuation (Fig. 3). The ionograms were manually scaled and then inverted into real-height electron density profiles using the above-described inversion technique and procedure.

Although VS measurements were carried out by the other ionosonde stations at Dourbes and Juliusruh on 3 October 2005, relatively low sampling rates of 1/10 and 1/15 min^{-1} were used since both stations are quite distant from the eclipse path and no significant eclipse effects were expected there.

2.2. Doppler data

The Doppler technique is a relatively simple method for detecting transient changes in the ionosphere (Davis and Baker, 1966) and capable of providing the data with relatively high time resolution. The measured Doppler shift between the transmitted radio signal of fixed frequency and signal reflected from the ionosphere is proportional to the rate of change of the signal phase path in the ionosphere. This change of phase path is mainly proportional to the vertical movement of the layer of reflection, which occurs approximately in the region where the plasma frequency equals the radio frequency. The Doppler shift may also depend on the compression or rarefaction of plasma, caused for example by a pulsating magnetic field (Sutcliffe and Poole, 1989). Two transmitters with slightly shifted frequencies and one receiver were in operation during the solar eclipse in Spain in 2005. One transmitter was installed in Teruel (40.35°N, 1.09°W), the other one in Granada (37.18°N, 3.58°W). The receiver for both signals was located in Balazote (38.87°N, 2.14°W). Assuming that the ionospheric reflection takes place in the middle between the transmitter and the receiver, then the reflection point of the Teruel's transmitter was on the eclipse path, whereas the reflection point of Granada's transmitter was about 200 km south of the path. A frequency of ~3.59 MHz was used but the received signal was converted to 80 Hz, amplified, digitized and processed. The data are visualized by means of Doppler shift spectrograms.

2.3. TEC data

Dual-frequency GPS observations can effectively be used to derive the TEC of the ionosphere (Jakowski,

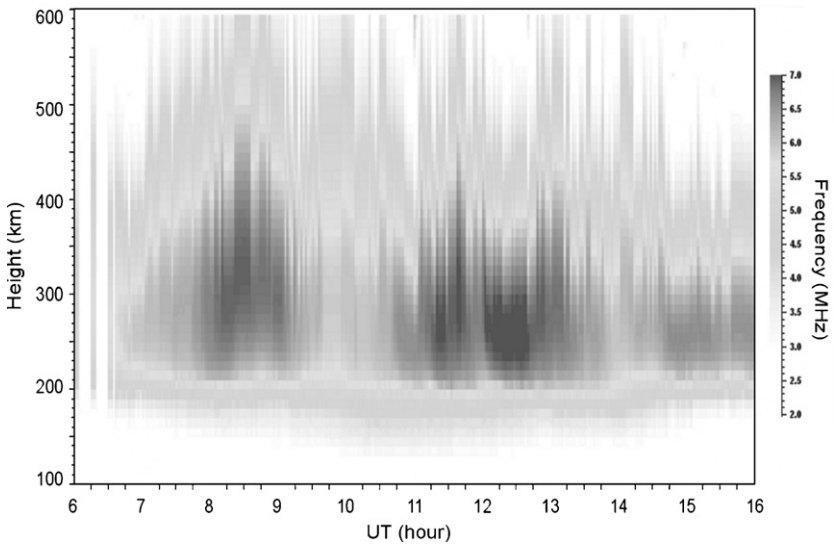

Fig. 3. Electron density reconstruction based on high-rate ionosonde sampling at Pruhonice (49.9°N, 14.5°E).

1996; Jakowski et al., 1999a). The dense European GPS network of the International GNSS Service (IGS) provides high-quality 30 s standard tracking data. Essentially based on these data, DLR have been operating, since 1995, a system for regularly processing ground-based GPS data and producing maps of the integrated electron content over the European and Polar regions (Jakowski, 1996). The GPS data, obtained mainly from the IGS network stations, allow the determination of slant TEC values along more than 100 satellite–receiver links. After calibration, the slant TEC data are mapped to the vertical by utilizing a mapping function based on a single-layer approximation at $h = 400$ km. Afterwards, the measurements are assimilated into a regional TEC model, NTCM (Jakowski et al., 1998), ensuring that the final map provides observation values near the points of measurements and adjusted model values over the areas without measurements. The routine TEC data used for the analysis are derived from the original GPS observations (30 s resolution) with a time resolution from 30 up to 600 s. Due to the assimilation procedure, the local noise is smoothed out by the weighted averaging over several measurements from different stations and/or satellites in the vicinity of the grid points of the map. The grid spacing is 2.5° in latitude and 5° in longitude directions. The accuracy of the reconstructions is in the order of $1–2 \times 10^{16}$ electrons/m^2 or 1–2 TEC units (TECU). European IGS and EUREF stations are permanently used to derive TEC and to construct TEC maps over Europe and both Polar areas (http://w3swaci.de/). In addition, local TEC data were deduced from individual GPS receiving stations of IGS in the vicinity of the eclipse path. The vertical TEC estimations provide calibrated TEC data along the GPS satellite links for elevation angles greater than 10° by using a standard technique (Ciraolo, 1993) in which the number of visible satellites from each GPS receiver allows considering only those satellites being closest to zenith. This restriction guarantees that the influence of eventual ionospheric inhomogeneities during the disturbed periods would be limited. The slant TEC data are then converted to equivalent vertical values at the sub-ionospheric point (Cander and Ciraolo, 2002), assuming a single-layer approximation of the ionosphere at an altitude of 400 km.

3. Vertical incidence sounding observations

The VS observations made at different European stations enable the comparison of solar eclipse effects with respect to the eclipse magnitude as observed from each station and station position/orientation to the annularity belt. A detailed look at the diurnal variations of the plasma frequency shows a clear reduction in the ionospheric F2 layer during the eclipse (Figs. 4 and 5). While the depletion is particularly strong over Ebro, it is not so at the more distant stations, Dourbes, where the depletion is observed at altitudes higher than 160 km, and Juliusruh, where the ionization loss is clearly visible only above 190 km. Such differences arise from the greater incidence angles of solar radiation at higher latitudes.

Gravity waves are known for contributing to the atmospheric dynamics, from the Earth's surface up to the mesosphere and lower thermosphere. The term acoustic-gravity waves stands for all wave motions in the atmosphere that satisfy the disperse relation (Hines, 1960). The periods of the gravity waves vary from minutes to hours. The importance of gravity wave motion lies in the energy redistribution within the atmospheric regions. Gravity waves are responsible for a great amount of variability in the atmosphere. They are almost always present in the atmosphere showing high day-to-day variability. It has been found that gravity waves are generated by many sources including topography, explosions, motion of large meteorological systems, wind shear, solar terminator motion, and others (Somsikov, 1995; Manzano et al., 1998; Martinis and Manzano, 1999; Fritts and Alexander, 2003; Fritts et al., 2006; Sauli et al., 2006b). Properties of the neutral waves, such as period and wavelength, are closely reflected by the electron density fluctuation due to the coupling of neutral and ionized components of the atmosphere. Once coupled, they can be observed as traveling ionospheric disturbances at ionospheric heights (Hooke, 1968; Djuth et al., 2004; Galushko et al., 1998; Taylor, 1998). The solar radiation flux cut-off during solar eclipses may act as an effective source of acoustic-gravity waves (Chimonas and Hines, 1970) and observation results have recently been reported (Fritts and Luo, 1993; Altadill et al., 2001). Observations relating the gravity waves to solar eclipses and proposed parameterization of the propagating pulses based on Fourier transformation have been reported in the works of Liu et al. (1998) and Altadill et al. (2001). Wave detection, based on wavelet transform, has been proposed recently by Sauli et al. (2006a, 2007).

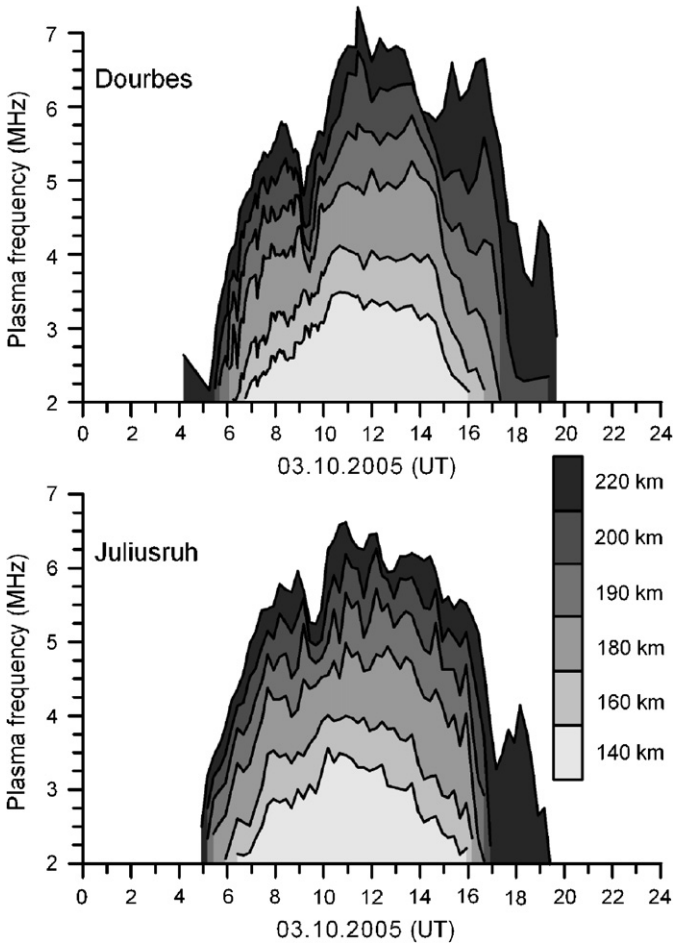

Fig. 4. Diurnal variation of plasma frequency at fixed heights at Dourbes (50.1°N, 4.6°E) and Juliusruh (54.6°N, 13.4°E).

3.1. Observations at the Ebro station

Time series of plasma frequency at fixed heights (140–220 km) were obtained at Ebro during the ionospheric campaign not only for the eclipse day but also for the previous and next days (Fig. 5). Electron density decreasing/increasing at the E and F1 layer, below 180 km, occurs simultaneously with the obscuration/de-obscuration of the Sun by the Moon. A similar reaction is observed also at F2-layer altitudes and above. Although these phenomena have been expected (Fig. 2), a delay of about 20–30 min is observed on the minimum plasma frequency values at different heights from 160 to 220 km. Moreover, a distinct oscillation activity (with a period of about 60 min) is detected in the F2 region, during and after the eclipse. This oscillation is not detected below 180 km height and is not observed in the neighboring days; hence it can be assumed that this is an ionospheric effect due to the solar eclipse, an indication of gravity wave generation.

Time series of reflection altitude values at fixed sounding frequencies were also obtained at Ebro during the eclipse, clearly showing changes in the height (Fig. 6). These changes are more pronounced during the main phase of the eclipse. A train of height oscillations starts at approximately 08:00 UT and further developed from 10:00 to 14:00 UT. The observed oscillation activity is clearer at higher altitudes, from 180 km up to the h_mF2, meaning that the oscillations are height coherent with a downward phase progression and with a period of about 60 min (Fig. 6, the white dashed lines). This time, oscillation activity is observed at lower altitudes, albeit not so clear and being of shorter period.

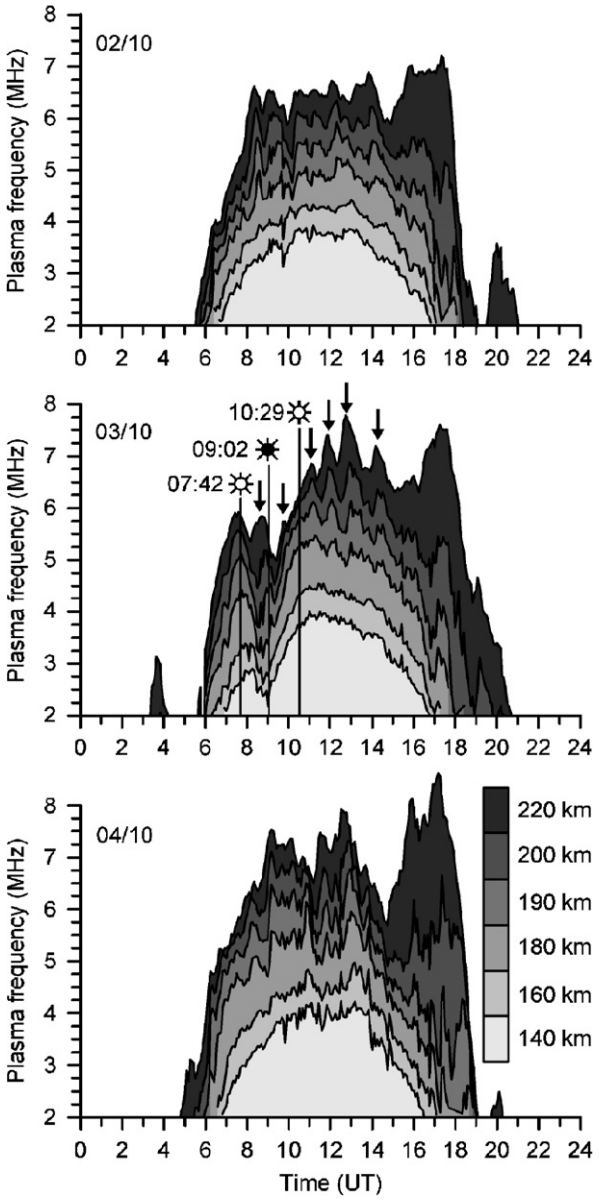

Fig. 5. Diurnal variations of plasma frequency at fixed "true" heights at Ebro observatory (40.8°N, 0.5°E). The moments of the start, maximum occultation, and end of solar eclipse (as seen at ground level) are clearly indicated on the plot of 3 October 2005. The wave crests are marked with arrows.

3.2. Observations at the Pruhonice station

In order to detect wave-like oscillations related to the solar eclipse event and trace wave-like structure through the ionosphere, a high-rate measurement campaign of vertical ionospheric sounding (every 2 min) has been carried out (Fig. 3). Apart from the obvious decrease of the plasma frequency at the start of the eclipse, wave-like oscillations occur during the eclipse. Below 180 km, the ionosphere reacts immediately to the solar disc obscuration, whereas, above 180 km, the electron density decreases with a delay of about 30 min. Besides the main decrease and later increase, shorter wave-like oscillations are well seen on the plot. These short-term oscillations are subject of further study. Our data consists of electron density variations, derived from true-height density profiles, presented at fixed heights in the range from 150 km up to 255 km with a step of 5 km. Obviously, the analysis is confined to altitudes below the F2-layer density peak.

First, we apply a high-pass filter on each time series of electron concentration to remove longer periods and focus on short-term oscillations. Then, we compute wavelet power spectrum at each altitude level, detect local energy maxima and their corresponding time position, period, amplitude and phase. From these maxima, we select only those that are persistent within sufficiently large range of heights and show smooth phase variation. The method, we used for estimation of gravity wave phase and packet velocities, is described by Sauli et al. (2006a, 2007), where wave packet selection, parameterization and computation of propagation characteristics is explained in details. Wavelet-based tools allow us to select pulses according to their occurrence time and to sort out those that occur before the event (Fig. 7).

Within ionospheric plasma, several coherent wave structures occur that can be attributed to the eclipse event according to their occurrence time. These structures appear in the plasma around the maximum obscuration, at 09:10 UT, and soon after the event, at 12:00 UT. One of the important characteristics of the gravity wave is the upward energy flow (positive packet velocity) when the phase travels downward with a negative phase velocity (Hines, 1960). Positive packet velocity, together with negative phase velocity, means that we observe gravity wave propagating upward. Indeed, the detected structures are characterized by a negative phase velocity and a positive packet velocity (Fig. 7). The upward motion (non-zero vertical component) indicates that source of the wave structure lays in the lower laying atmospheric regions. A mechanism of wave generation by cooling of ozone in the lower laying atmosphere was proposed by Fritts and Luo (1993). In such a case, the propagating structure progress upward within ionospheric heights. Another possible mechanism

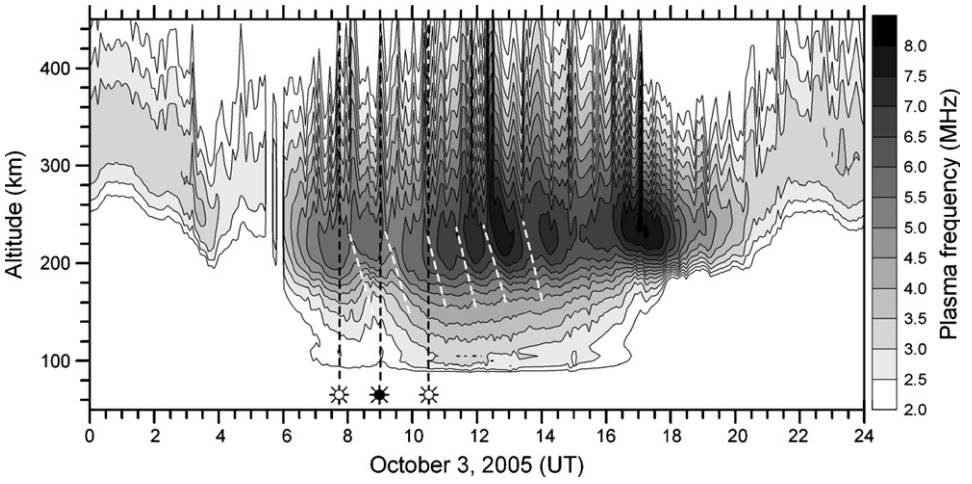

Fig. 6. Cross-section contour plots of electron density as function of time and height, Ebro observatory, 3 October 2005.

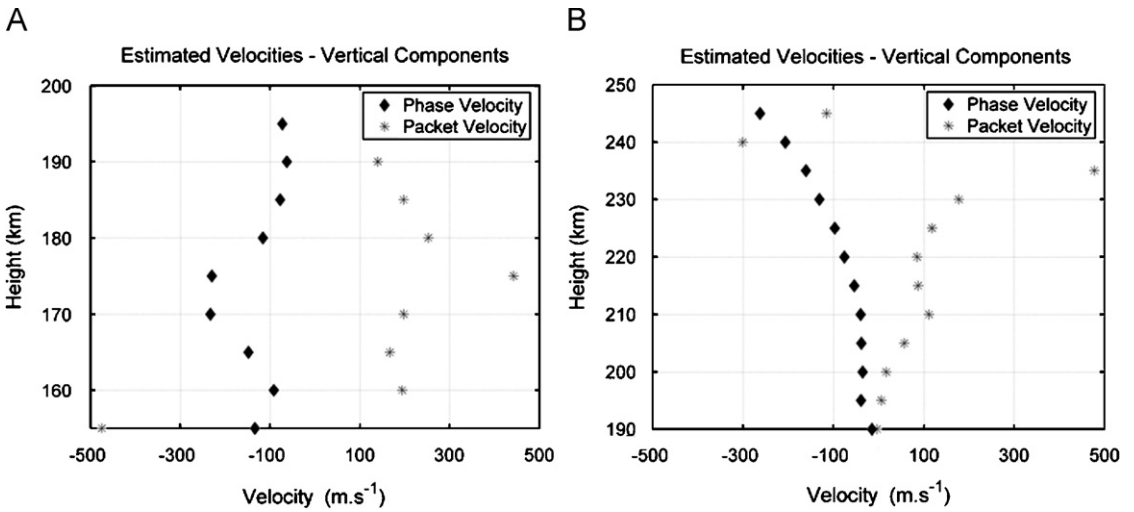

Fig. 7. Estimated packet and phase velocities. Panel A: Gravity wave with period ~43 min occurring around 9 h 10 min (maximum eclipse phase). Panel B: Gravity wave with period ~65 min detected slightly after 12 h (after eclipse event).

is the formation of a bow structure due to the supersonic motion of the Moon shadow (Chimonas and Hines, 1970). Such a wave structure propagates obliquely from the eclipsed region and may be detected as upward propagating structure at ionospheric heights. Due to the time occurrence (maximum phase, after eclipse) of wave structures and their propagation velocities, we suppose that the detected wave-like oscillations are produced by the solar eclipse. The source of these waves may be found in the propagation of a shock wave and the abrupt decrease of solar heating in the lower lying atmosphere.

4. Doppler observations

To study the transient phenomena on short time scales, we also used Doppler shift measurements of continuous sounding at a frequency of 3.59 MHz. The resulting Doppler shift spectrograms, recorded during the eclipse on 3 October 2005, are given in Fig. 8. One of the spectrograms (panel A) corresponds to the signal which point of reflection is above the eclipse path (of maximum obscuration). The other spectrogram (panel B) shows the evolution of the Doppler shift of the signal reflected about 200 km south of the eclipse path. The

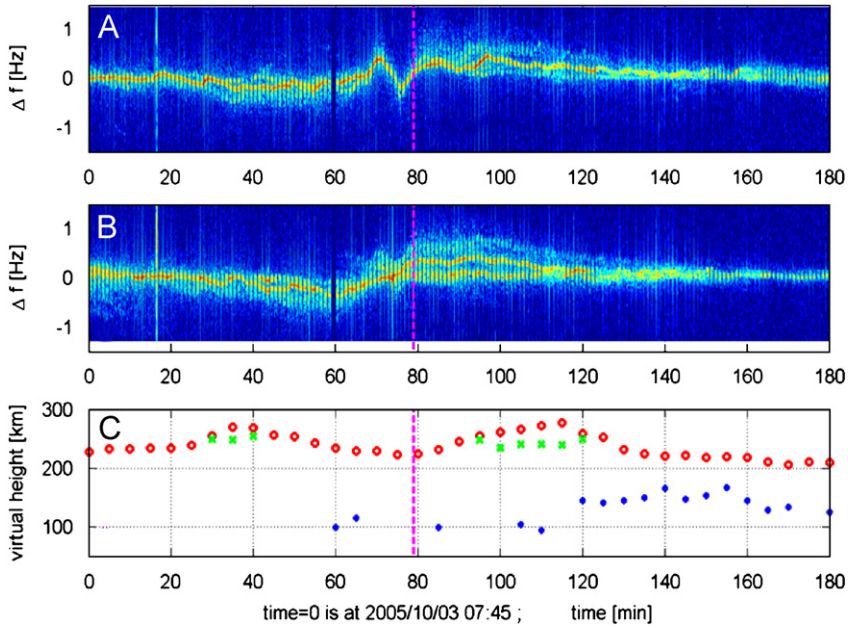

Fig. 8. Doppler 3.59 MHz frequency measurements and VS measurements carried out in Spain during the solar eclipse on 3 October 2005 from 07:45 to 10:45 UT. Panel A: Doppler shift spectrogram of the signal having a reflection point on the eclipse path (of maximum obscuration). Panel B: Doppler shift spectrogram of the signal having a reflection point about 200 km south of the eclipse path. Panel C: VS virtual height measurements at the Ebro observatory. The red circles indicate the ordinary waves reflecting from the ionospheric F-layer, the green crosses are used for indicating the extraordinary waves reflecting from the F-layer below the reflection of ordinary waves, and the blue diamonds indicate the reflection from the semi-transparent sporadic E layer.

maximum obscuration occurred at about 09:04 UT and it is marked with a vertical dashed line (magenta). Both signals experienced a slow decrease of the frequency during the initial phase of the eclipse and a similarly slow increase after that, just before the main phase of the eclipse. This increase corresponds to the increase of the plasma density and the lowering of the reflection layer. Additionally, a superimposed short period wave-like disturbance was observed on the signal reflected in the band of maximum eclipse. When the eclipse approached its maximum, a short but distinct transient negative Doppler shift occurred, suggesting the occurrence of a transient upward movement of the reflection layer and a corresponding depletion of the ionospheric plasma density. However, these effects were not observed on the signal reflected outside the band of maximum eclipse. This is different from the results obtained by Jones et al. (2004) who reported short-term negative Doppler shifts on several signals reflected north of the band of total eclipse.

To estimate the virtual height of a 3.6 MHz signal reflection, VS measurements from Ebro, the station closest to the eclipse path, have been used (Fig. 8, panel C). The ionograms show that the signal reflected from the F2 layer until 09:30 UT (the 105th min). The sounding frequency was very close to the critical frequency of the F1 layer (f_oF1) from 09:30 to 09:45 UT. After that, the signal reflected from the F1 layer. A semi-transparent sporadic E layer, which did not probably affect the reflection height, was also present from 09:45 UT (the 120th min) onwards. The amplitudes of waves reflected from the F1 layer are smaller than the amplitudes of waves reflected from the F2 layer (Jones et al., 2004). The bifurcated trace (Fig. 8, panel B) seems to correspond to the reception of extraordinary waves in the ionograms (Fig. 8, panel C); the small discrepancies in time can be explained with the different locations of the reflection points.

5. TEC measurements

The TEC provides an integral measure of the vertical ionospheric electron density. Thus, during a solar eclipse, TEC provides information about the total ionization loss of the ionosphere as a consequence of the reduced photo ionization. This type of measurement is not very sensitive to the

plasma redistribution processes and local effects, contrary to the VS technique. On the other hand, the VS measurements may not provide accurate information about the total ionization loss; principally, the TEC value corresponds better to the solar-radiation function. GPS TEC measurements in Spain show a significantly reduced ionization during the annular eclipse on 3 October 2005 (Fig. 9). Although the dip in ionization is difficult to estimate because of the natural variability of TEC, a rough estimation indicates a total plasma loss of 20–30%.

Nowadays, the existence of dense GPS receiver networks offers a good opportunity to monitor the total loss of ionospheric ionization during solar eclipses on a local or regional scale. TEC maps also enable studies of the horizontal distribution and transport of the ionospheric plasma. Reliable three-dimensional reconstructions of the plasma distribution can be expected in the near future when additional height information is provided from ionosondes and/or GPS radio occultation measurements onboard LEO satellites (Stolle et al., 2003). To highlight the TEC variations, it is useful to construct maps of the differential TEC value, $\Delta TEC = (TEC - TEC_{med})/TEC_{med} \times 100\%$. In this way, the ionospheric dynamics during the solar eclipse becomes quite obvious (Fig. 10). It is impressive to see the large depletion zone around the shadow spot and its movement, with a supersonic speed, along the eclipse path. Generally, the depletion is about 30% inside the shadow which agrees with other local measurements. Judging from the maps for 09:00 and 10:00 UT, the depletion zone extends far into the high latitudes. The large extension of this plasma depletion zone is confirmed by other plots of the TEC percentage deviations from monthly medians, along the 0°E and 15°E meridians (Fig. 11). Such extension can only be explained if plasma transport processes are activated during the eclipse. The solar incidence angle influences the level of plasma depletion, as proved by the VS measurements at different stations (Figs. 4 and 5). The depletion is maintained for hours showing that the recovery of the plasma density is decoupled from the obscuration function.

TEC measurements can also be used to detect AGW. For the purpose, 1 Hz sampled dual-frequency GPS carrier phases were used during the target campaign organized by IGS on the occasion of the solar eclipse on 11 August 1999 (Feltens and Noll, 1999). Usually, the uncalibrated differential TEC data can provide more valuable information about the wave-like phenomena than the final TEC maps because the map's grid spacing may interfere

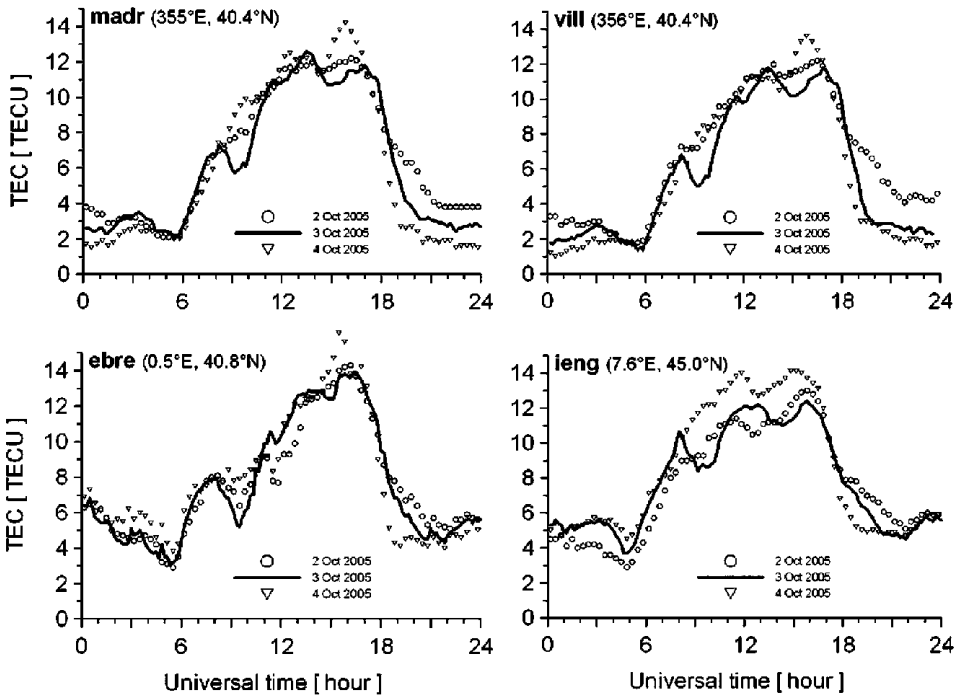

Fig. 9. Comparison of TEC measurements at different GPS stations, carried out on 2–4 October 2005 at different GPS receiver stations in Spain. Notice the significant plasma loss of 20–30% during the eclipse on 3 October 2005.

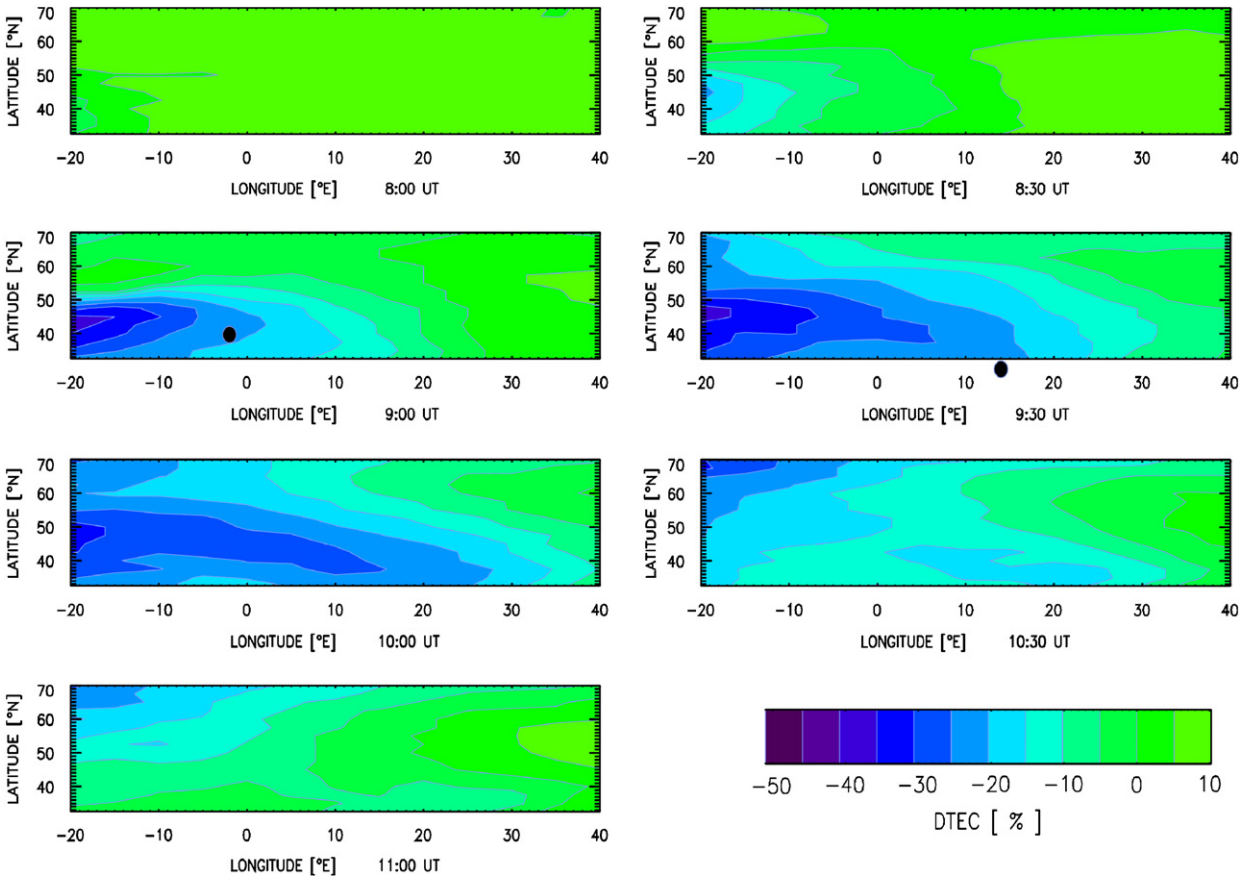

Fig. 10. Sequential maps of the differential TEC (percentage deviations from monthly medians) over Europe during the solar eclipse on 3 October 2005 (the shadow spot is marked by a solid circle).

with the wavelength. Also, to remove the bias effects, the TEC rate must also be computed. Furthermore, the GPS TEC measurement data were filtered at various periods: 10–30, 20–60, 40–80, and 60–120 min. As Fig. 12 shows, no enhanced wave activity was detected during the eclipse on 3 October 2005. This result is representative since similar observations from other GPS stations using other satellite links could not be able to detect the AGW activity on this occasion.

6. Discussion

Solar eclipses affect the Earth's atmosphere and ionosphere in a complex manner. The atmospheric reactions include thermospheric cooling, neutral winds, and composition changes (Mueller-Wodarg et al., 1998) that set up the background and influence for the ionospheric response. A considerable portion of the ionizing radiation at shorter wavelengths stems from the solar corona, which is not fully obscured by the Moon (Davis et al., 2001). That means that although the photo ionization is reduced during eclipses, it is not completely blocked. While the bottom-side ionosphere is mainly controlled by the local solar radiation, the F2 layer and the top-side ionosphere are less prone to the radiation and are rather influenced by processes of plasma redistribution (Cheng et al., 1992).

Perturbation processes may be the reason behind the enhanced local electron density just before the obscuration function reaching its maximum at 10:18 UT on 11 August 1999 and at 09:02 UT on 3 October 2005, as observed at the Ebro ionosonde station (Fig. 13). The increase on 3 October 2005 is much more pronounced which suggests that, apart from the eclipse effects, the terminator passage shortly before the eclipse may also play a role here. The moving terminator is known to be able of causing irregularities during sunrise and sunset periods (Somsikov, 1995).

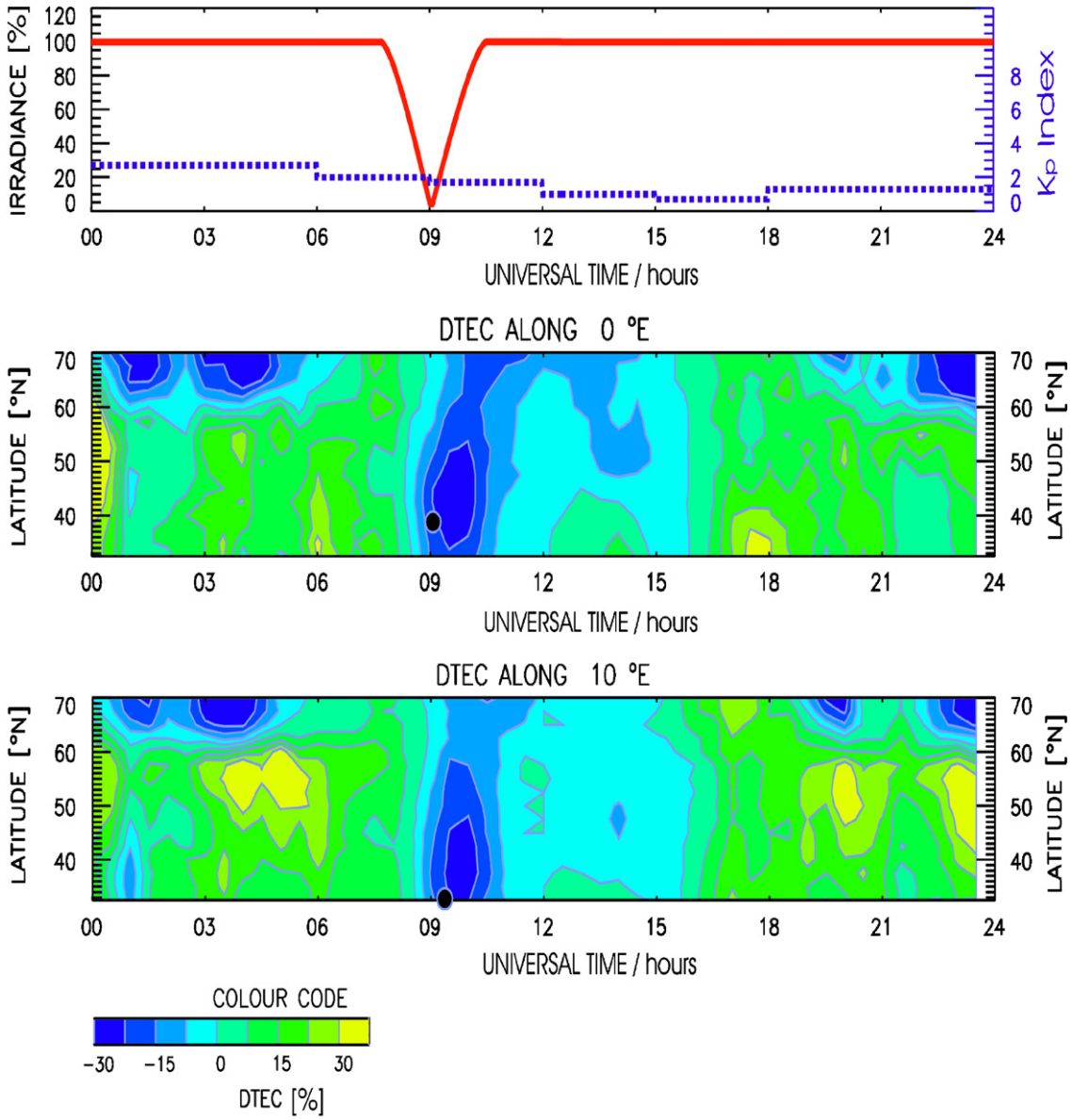

Fig. 11. Diurnal variations of the differential TEC (%) on 3 October 2005 within the latitudinal range from 30°N to 70°N along the 0°E (middle panel) and 15°E (bottom panel) meridians. The obscuration function is plotted for 0°E in the top panel.

Considering the response time of the ionospheric ionization to changes in the obscuration function, it is expected that the lower ionosphere, characterized by strong recombination processes, responds faster than the ionosphere at higher altitudes where the plasma life-time grows and the diffusion processes need some time to come into effect. This behavior is clearly seen by the increasing delay of the depletion minimum with increasing altitude (Fig. 13, dashed line). At the location of the Ebro station, the time delay is about 25 min at about 200 km. The time delay seen in the TEC measurements is in the same order (Fig. 15). This finding corresponds very well with the modeling results obtained for the thermospheric temperatures and winds during the solar eclipse on 11 August 1999 (Mueller-Wodarg et al., 1998). However, while Afraimovich et al. (2002) report very short response times of only a few minutes, Tsai and Liu (1999) found much longer response times of up to 120 min when studying the solar eclipses on 24 October 1995 and 9 March 1997 at low latitudes. It should be noticed at this point

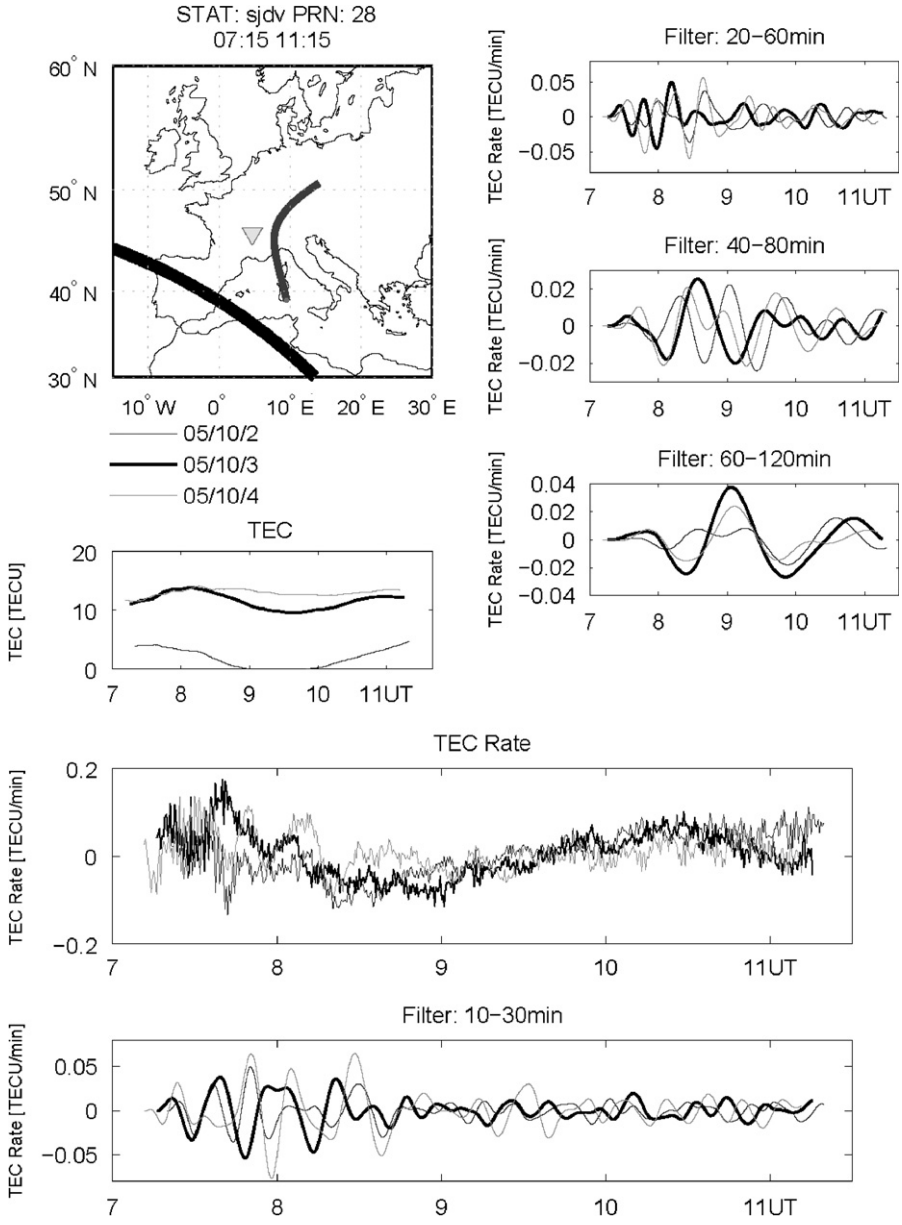

Fig. 12. Original and filtered link-related slant TEC rate during the eclipse on 3 October 2005. The ray path geometry is seen at the upper left panel.

that the low-latitude ionosphere is strongly influenced by dynamic processes related to the equatorial anomaly, i.e. the transport processes dominate the photochemical processes.

When studying the ionospheric response to solar eclipses, a question arises whether the gravity waves are generated due to the fast moving shadow of the Moon (Chimonas and Hines, 1970). Since the geomagnetic activity during the eclipses on 11 August 1999 and on 3 October 2005 was low ($a_p \leqslant 12$), the strong ionospheric perturbations of magnetospheric origin like electric fields or storm-induced winds are excluded as driving forces for wave-like oscillations. Both the VS and Doppler observations indicate the occurrence of significant plasma oscillations. Such oscillations, having a period of about 1 h, are clearly seen in the plasma frequency and in the altitude variations of the F region. The origin is located in the transition region between the F1 and F2 layers, somewhere below

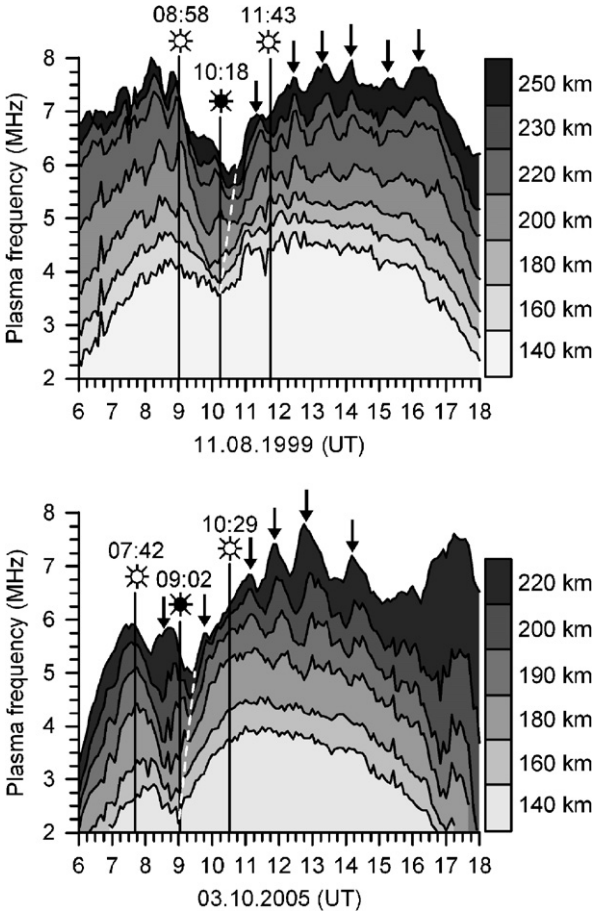

Fig. 13. Comparison of the vertical structure of the plasma frequency and its time response above the Ebro station obtained during the total eclipse on 11 August 1999 and during the annular eclipse on 3 October 2005. The response is delayed up to 25 min at higher altitudes (cf. the dashed line). The oscillation amplitudes are marked with arrows.

180 km altitude. From there, the wave propagates vertically, thus pushing the energy upwards while its phase progression goes downwards (Fig. 6). This somewhat differs from the observations during the solar eclipse of 11 August 1999 when it was found that the wave activity, originated at about 180 km altitude, propagates upward and downward simultaneously (Altadill et al., 2001). We believe that a similar wave activity source can play a role also during the eclipse on 3 October 2005. Further work is needed to get an exact understanding of this phenomenon.

In agreement with the observations at Ebro, the Pruhonice observation also indicates the occurrence of gravity waves during eclipses. However, the analysis of the Pruhonice data led to a different localization of the wave source. It was speculated that the waves originate from the middle atmosphere (e.g. ozone layer) well below the ionosphere. The reason for the different results remains unclear. The most plausible reason for the differences between both statistics is in the different distances to the eclipse path. Also, the solar incidence angle is higher at Pruhonice than at the Ebro station.

Due to its integral nature, the TEC value reflects wave-like phenomena in a quite different manner than any of the VS quantities do. Nevertheless, gravity waves are still visible in TEC data if the wave amplitude is large enough and the ray path geometry determined by the positions of the GPS satellite and the receiving ground stations does not allow canceling out the wave signatures while integrating electron density along the ray path (Davis and Da Rosa, 1970; Jakowski et al., 1983, 2001; Tsai and Liu, 1999; Rashid et al., 2006). In many cases, the generation mechanism of these TIDs remains unclear due to the non-negligible geomagnetic activity. Since the wave activity observed in TEC at different European GPS stations on 11 August 1999 started earlier than the solar eclipse and strong weather fronts appeared over Europe, it was concluded that tropospheric sources should also be taken into account when discussing sources of gravity waves occurring during solar eclipses (Jakowski et al., 2001).

The examination of the GPS data with respect to the increased wave activity during the annular eclipse on 3 October 2005 did not produce evidences of such activity from the TEC data. In this respect, it should be noted that TIDs are frequently observed in the TEC data, thus contributing to the natural variability of the TEC value. Considering also the integral feature of TEC, it is assumed that either the amplitudes of the propagating waves through the ionospheric plasma are too small or the waves are mainly vertically structured. The latter may produce clear patterns in the local VS data but may also lead to canceling out plasma variations in the TEC data. Nevertheless, although enhanced wave activity was not observed via TEC, it was revealed that the eclipse caused significant changes in the total ionization level (Figs. 9–11). We could learn something about the profile shape variations during the eclipse by combining VS and TEC measurements to calculate the equivalent slab thickness, $\tau = \mathrm{TEC}/N_{\mathrm{m}}\mathrm{F2}$. The slab thickness is a valuable measure of the width of the electron density profile, which is expected to grow up during the obscuration (Fig. 2). Indeed, the slab thickness increases by about 20–30 km when the solar

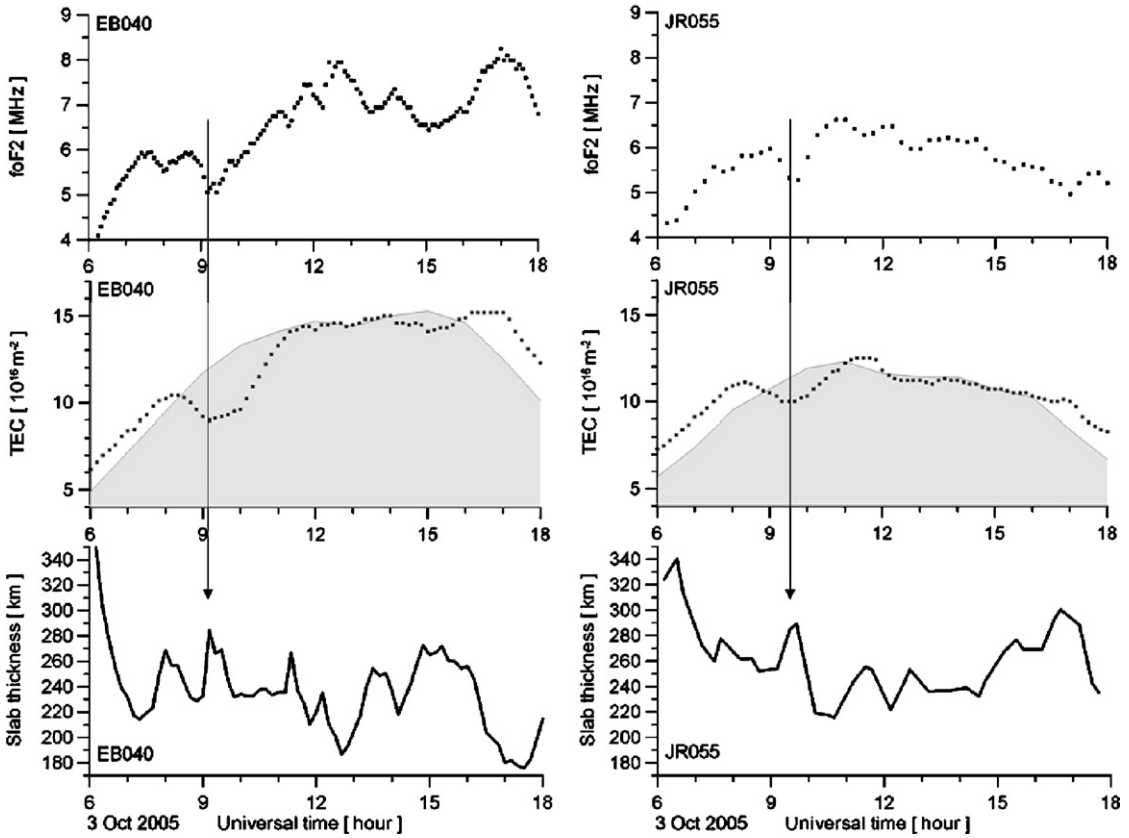

Fig. 14. Slab thickness variations over the ionosonde stations Ebro and Juliusruh during the solar eclipse on 3 October 2005.

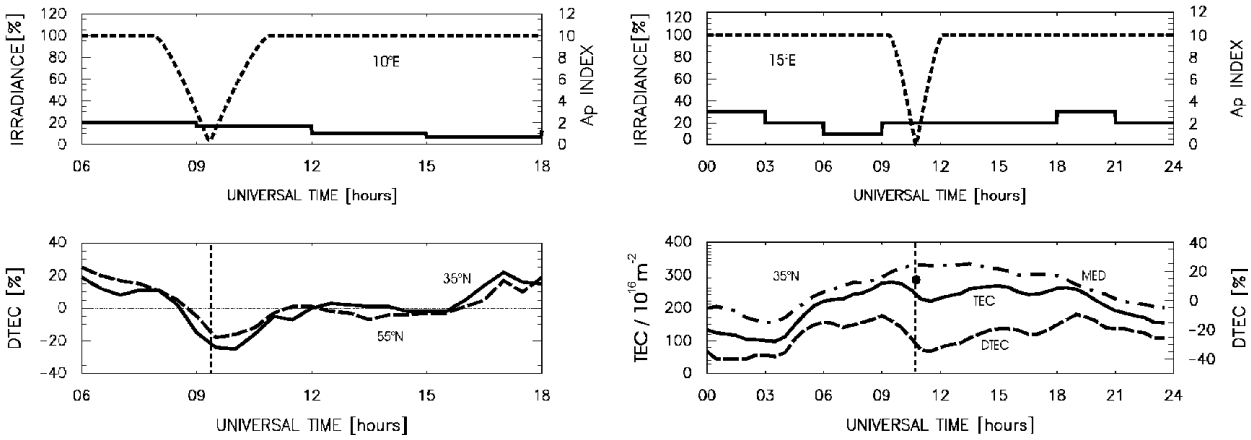

Fig. 15. Ionospheric depletion of the total ionization measured by TEC during the solar eclipses on 3 October 2005 (left panel) and on 11 August 1999 (right panel).

radiation was reduced during the first phase of the eclipse (Fig. 14). On the one hand, the peak density height is expected to increase due to plasma loss in the bottom-side ionosphere. On the other hand, the thermospheric cooling and vertical winds (Mueller-Wodarg et al., 1998) may prevent this and actually cause the opposite reaction. The h'F2 data at Pruhonice did not show remarkable changes that can be closely related to the eclipse. However, the cooling could not prevent the increase of the slab thickness because of the photochemical and recombination processes in the bottom-side ionosphere.

The enhanced slab thickness during the first phase yields evidences for a delayed depletion of the topside ionosphere. After the maximum obscuration, the slab thickness decreased rapidly, a fact which should be related to the eclipse-generated cooling of the thermosphere.

The TEC observations show a significant reduction of several TEC units. Whereas the total plasma depletion during the eclipse on 11 August 1999 (Fig. 15) reached 40% ($TEC_{max} \approx 25$–30 TECU), the depletion was about 30% on 3 October 2005 ($TEC_{max} \approx 15$–20 TECU). This is in agreement with TEC observations reported earlier (Tsai and Liu, 1999; Jakowski et al., 1983, 1999b, 2001; Rashid et al., 2006). The difference between the October and the August eclipses may be explained with the different local times of the maximum obscuration. The strongest reduction is expected to be observed around noon, i.e. at the eclipse on 11 August 1999. Furthermore, the eclipse on 3 October 2005 does not reach 100% obscuration. The degree of depletion is confirmed by the differential TEC maps normalized to the corresponding monthly medians (Figs. 11 and 16). Notice that the depletion covers a large area up to the high latitudes. It is also interesting that both eclipses show different latitudinal depletion patterns over time. Whereas on 11 August 1999, the depletion zone extends towards lower latitudes with a long lasting depletion effect at the lower border of the map (Fig. 16), on 3 October 2005, the depletion zone extends towards higher latitudes (Fig. 11). This effect is remarkable because the eclipse path on 11 August 1999 is further north than the eclipse path on 3 October 2005. Considering the eclipse geometry, on 3 October 2005, the obscuration maximum appears at higher latitudes later (http://sunearth.gsfc.nasa.gov/eclipse/SEmono/ASE2005/ASE2005.html). On 11 August 1999, the

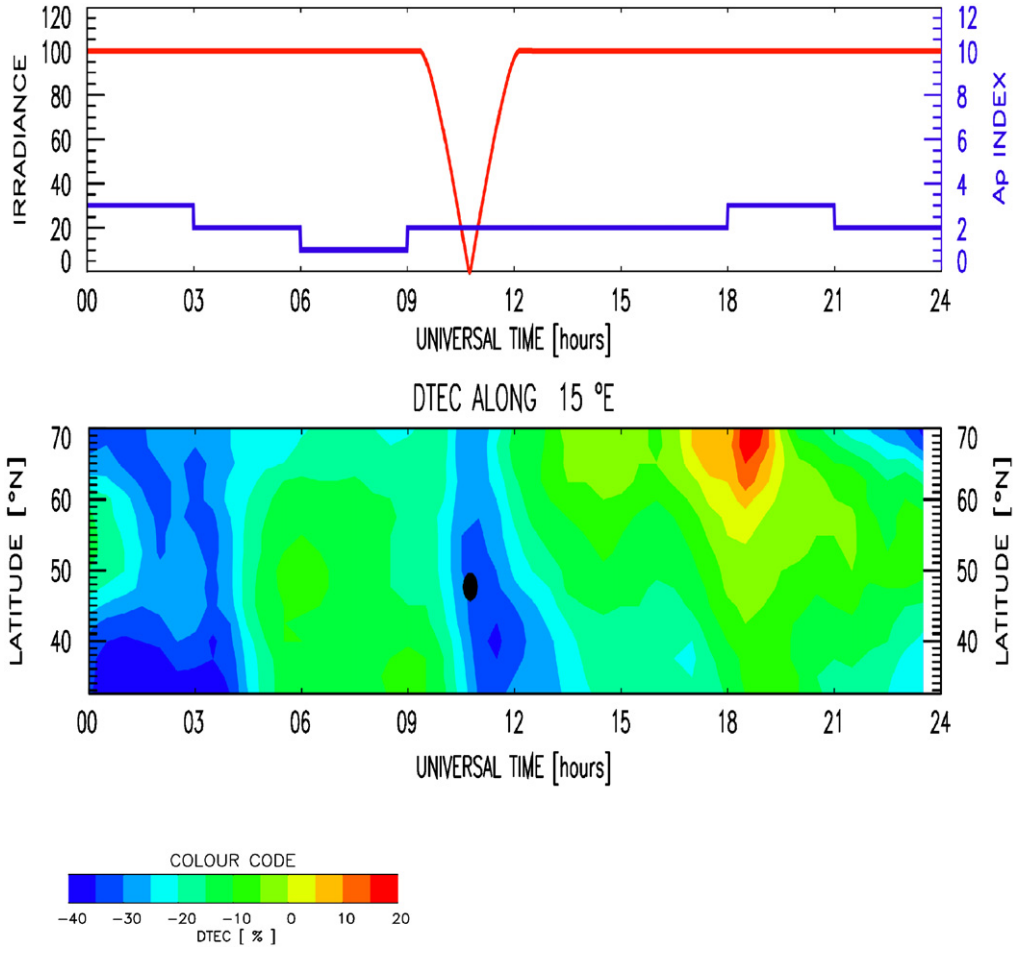

Fig. 16. Diurnal variations of the differential TEC (%) on 11 August 1999 within the latitudinal range from 30°N to 70°N along the15°E meridian. The corresponding obscuration function is plotted in the top panel.

maximum obscuration occurs at nearly the same time at high latitudes, in agreement with the observations (Fig. 16). The reason for the different temporal behavior of the depletion zone at both eclipses remains unclear. Apart from the different eclipse geometry, obviously the horizontal transport processes have to be taken into account. Seasonal and local time differences in the thermospheric wind system also influence the spatial and temporal behavior of the recovery process. Simulations may help the understanding of this complex interplay of cooling, photochemistry and transport processes during eclipses.

7. Conclusions

The ionospheric behavior during the annular eclipse on 3 October 2005 has been investigated using VS, High-frequency (HF) Doppler, and TEC measurements. The results can be summarized as follows.

The total ionization, as estimated by the TEC, reduces by approximately 30%. This is in agreement with earlier findings for other eclipses.

The VS and HF Doppler measurements, carried out in proximity of the eclipse path, indicate the generation of AGW. It is assumed that waves, having wave periods in the order of 60 min, originate in the thermosphere at around 180 km altitude. The Pruhonice data also show a wave activity with periods of about 60 min but indicate a source region well below the ionosphere, somewhere in the middle atmosphere.

Since the TEC measurements were not able to detect enhanced wave activity on a larger scale, it is assumed that the amplitudes of the propagating waves through the ionospheric plasma are small and/or are mainly vertically structured. The latter produces strong pattern in the local VS data and leads to canceling out plasma variations in TEC.

The ionospheric response to the obscuration function is delayed by 20–30 min and is increasing with altitude. This is in agreement with earlier observations made during the solar eclipse on 11 August 1999.

The equivalent slab thickness was found to increase by approximately 20 km during the initial phase of the solar eclipse on 3 October 2005. The thermospheric cooling seems to be in competition with this increase, probably leading to a slab thickness decrease in the latter stages of the eclipse.

The different dynamic features of the latitudinal dependence of the temporal behavior of the depletion zone observed during the eclipses on 3 October 2005 and 11 August 1999, need further investigation. It is assumed that besides the eclipse geometry, thermospheric winds also contribute to the observed depletion pattern.

Acknowledgments

This research has been funded by the German State Government of Mecklenburg-West Pomerania under Grant V230-630-08-TIFA-334. The work of the Ebro team is partialy supported by the Spanish Project REN2003-08376-C02. The work is supported by Grant nos. 205/07/1367 and 205/06/1619 of the Grant Agency of the Czech Republic and Grants nos. IAA300420504 and 1QS300120506 of the Grant Agency of the ASCR. The authors are grateful to the International GNNS Service for enabling the use of measurements of numerous GPS stations from the European Network. The work was initiated and supported by the European COST 296 Action.

References

Afraimovich, E.L., Kosogorov, E.A., Lesyuta, O.S., 2002. Effects of the August 11, 1999 total solar eclipse as deduced from total electron content measurements at the GPS network. Journal of Atmospheric and Solar–Terrestrial Physics 64, 1933–1941.

Altadill, D., Sole, J.G., Apostolov, E.M., 2001. Vertical structure of a gravity wave like oscillation in the ionosphere generated by the solar eclipse of August 11, 1999. Journal of Geophysical Research 106, 21419–21428.

Baron, M.J., Hunsuker, R.D., 1973. Incoherent scatter radar observations of the auroral zone ionosphere during total solar eclipse of July 10, 1972. Journal of Geophysical Research 78, 7451–7460.

Cander, Lj.R., Ciraolo, L., 2002. First step towards specification of plasmaspheric–ionospheric conditions over Europe on-line. Acta Geodaetica et Geophysica Hungarica 37 (2–3), 153–161.

Cheng, K., Huang, Y.N., Chen, S.W., 1992. Ionospheric effects of the solar eclipse of September 23, 1987, around the equatorial anomaly crest region. Journal of Geophysical Research 97, 103–111.

Chimonas, G., Hines, C.O., 1970. Atmospheric gravity waves induced by a solar eclipse. Journal of Geophysical Research 75, 875.

Ciraolo, L., 1993. Evaluation of GPS L2-L1 biases and related daily TEC profiles. In: Proceedings of the GPS/Ionosphere Workshop, Neustrelitz, pp. 90–97.

Cohen, E.A., 1984. The study of the effect of solar eclipses on the ionosphere based on satellite beacon observations. Radio Science 19, 769–777.

Davis, K., Baker, D.M., 1966. On frequency variations of ionospherically propagated HF radio signals. Radio Science 1, 545–556.

Davis, M.J., Da Rosa, A.V., 1970. Possible detection of atmospheric gravity waves generated by the solar eclipse. Nature 226, 1123.

Davis, C.J., Clarke, E.M., Bamford, B.A., Lockwood, M., Bell, S.A., 2001. Long term changes in EUV and X-ray emissions

from the solar corona and chromosphere as measured by the response of the Earth's ionosphere during total solar eclipses from 1932–1999. Annales Geophysicae 19, 263–273.

Djuth, F.T., Sulzer, M.P., Gonzales, S.A., Mathews, J.D., Elder, J.H., Walterschied, R.L., 2004. A continuum of gravity waves in the Arecibo thermosphere? Geophysical Research Letters 31, L16801.

Farges, T., Le Pichon, A., Blanc, E., Perez, S., Alcoverro, B., 2003. Response of the lower atmosphere and ionosphere to the eclipse of August 11, 1999. Journal of Atmospheric and Solar–Terrestrial Physics 65, 717–726.

Feltens, J., Noll, C., 1999. GPS data collected during August 1999 solar eclipse. CDDIS Bulletin 14, 5.

Fritts, D.C., Alexander, M.J., 2003. Gravity dynamics and effects in the middle atmosphere. Reviews of Geophysics 41, doi:10.1029/2001RG000106, 3.1–3.64.

Fritts, D.C., Luo, Z., 1993. Gravity wave forcing in the middle atmosphere due to reduced ozone heating during a solar eclipse. Journal of Geophysical Research 98 (D2), 3011–3021.

Fritts, D.C., Vadas, S.L., Wan, K., Werne, J.A., 2006. Mean and variable forcing of the middle atmosphere by gravity waves. Journal of Atmospheric and Solar–Terrestrial Physics 68, 247–265.

Galushko, V.G., Paznukhov, V.V., Yampolski, Y.M., Foster, J.C., 1998. Incoherent scatter radar observations of AGW/TID events generated by the moving solar terminator. Annales Geophysicae 16, 821–827.

Hines, C.O., 1960. Internal atmospheric gravity waves at ionospheric heights. Canadian Journal of Physics 38, 1441–1481.

Hooke, W.H., 1968. Ionospheric irregularities produced by internal atmospheric gravity waves. Journal of Atmospheric and Solar–Terrestrial Physics 30, 795–823.

Huang, X., Reinisch, B.W., 1996. Vertical electron density profiles from the digisonde network. Advances in Space Research 18 (6), 121–129.

Huang, C.R., Liu, C.H., Yeh, K.C., Lin, K.H., Tsai, W.H., Yeh, H.C., Liu, J.Y., 1999. A study of tomographically reconstructed ionospheric images during a solar eclipse. Journal of Geophysical Research 104 (A1), 79–94.

Jakowski, N., 1996. TEC monitoring by using satellite positioning systems. In: Kohl, H., Rüster, R., Schlegel, K. (Eds.), Modern Ionospheric Science. EGS, Katlenburg-Lindau, Germany, pp. 371–390.

Jakowski, N., Bettac, H.D., Lazo, B., Palacio, L., Lois, L., 1983. The ionospheric response to the solar eclipse of 26 February 1979 observed in Havana/Cuba. Physica Solariterrestris 20, 110–116.

Jakowski, N., Sardon, E., Schlueter, S., 1998. GPS-based TEC observations in comparison with IRI95 and the European TEC model NTCM2. Advances in Space Research 22 (6), 803–806.

Jakowski, N., Schlueter, S., Sardon, E., 1999a. Total electron content of the ionosphere during the geomagnetic storm on 10 January 1997. Journal of Atmospheric and Solar–Terrestrial Physics 61, 299–307.

Jakowski, N., Schlueter, S., Heise, S., Feltens, J., 1999b. Satellite technology glimpses ionospheric response to solar eclipse. EOS transactions, vol. 80. American Geophysical Union, 21 December 1999, p. 51.

Jakowski, N., Heise, S., Wehrenpfennig, A., Schlueter, S., 2001. Total electron content studies of the solar eclipse on 11 August 1999, CD-ROM. In: Proceedings of the IBSS, Boston, 4–6 June 2001, pp. 279–283.

Jones, T.B., Wright, D.M., Milner, J., Yeoman, T.K., Reid, T., Chapman, P.J., Senior, A., 2004. The detection of atmospheric waves produced by the total solar eclipse of 11 August 1999. Journal of Atmospheric and Solar–Terrestrial Physics 66, 363–374.

Liu, J.Y., Hsiao, C.C., Tsai, L.C., Liu, C.H., Kuo, F.S., Lue, H.Y., Huang, C.M., 1998. Vertical Phase and Group velocities of internal gravity waves derived from ionograms during the solar eclipse of 24 October 1995. Journal of Atmospheric and Solar–Terrestrial Physics 60, 1679–1686.

Manzano, J.R., Radicella, S.M., Zossi de Artigas, M.M., Filippi de Manzano, A.N., Cosio de Ragone, A.H., 1998. Troposphere–ionosphere interaction during tropospheric mesoscale convective complexes events. Journal of Atmospheric and Solar–Terrestrial Physics 60, 585–594.

Martinis, C.R., Manzano, J.R., 1999. The influence of active meteorological systems on the ionospheric F-region. Annali di Geofisica 42 (1), 1–7.

McPherson, B., Gonzalez, S.A., Sulzer, M.P., Bailey, G.J., Djuth, F., Rodriguez, P., 2000. Measurements of the topside ionosphere over Arecibo during the total solar eclipse of February 26, 1998. Journal of Geophysical Research 105, 23055–23067.

Mueller-Wodarg, I.C.F., Aylward, A.D., Lockwood, M., 1998. Effects of a mid-latitude solar eclipse on the thermosphere and ionosphere: a modelling study. Geophysical Research Letters 25, 3787–3790.

Rashid, Z.A.A., Momani, M.A., Sulaiman, S., Ali, M.A.M., Yatim, B., Fraser, G., Sato, N., 2006. GPS ionospheric TEC measurement during the 23rd November 2003 total solar eclipse at Scott Base Antarctica. Journal of Atmospheric and Solar–Terrestrial Physics 68, 1219–1236.

Reinisch, B.W., Huang, X., Galkin, I.A., Paznukhov, V., Kozlov, A., 2005. Recent advances in real-time analysis of ionograms and ionospheric drift measurements with digisondes. Journal of Atmospheric and Solar–Terrestrial Physics 67, 1054–1062.

Sauli, P., Abry, P., Boska, J., Duchayne, L., 2006a. Wavelet characterisation of ionospheric acoustic and gravity waves occurring during the solar eclipse of August 11, 1999. Journal of Atmospheric and Solar–Terrestrial Physics 68, 586–598.

Sauli, P., Abry, P., Altadill, D., Boska, J., 2006b. Detection of the wavelike structures in the F-region electron density: two station measurements. Studia Geophysica and Geodetica 50, 131–146.

Sauli, P., Roux, S., Abry, P., Boska, J., 2007. Acoustic-gravity waves during solar eclipses: detection and characterisation using wavelet transforms. Journal of Atmospheric and Solar–Terrestrial Physics 69 (17–18), 2465–2484.

Somsikov, V.M., 1995. On the mechanisms for the formation of atmospheric irregularities in the solar terminator region. Journal of Atmospheric and Terrestrial Physics 57 (1), 75–83.

Stolle, C., Schlueter, S., Jacobi, Ch., Jakowski, N., 2003. 3-Dimensional ionospheric electron density reconstruction based on GPS measurements. Advances in Space Research 31 (8), 1965–1970.

Sutcliffe, P.R., Poole, A.W.V., 1989. Ionospheric Doppler and electron velocities in the presence of ULF waves. Journal of Geophysical Research 94, 13505–13514.

Taylor, M.J., 1998. Possible evidence of gravity wave coupling into the midlatitude F region ionosphere during seek campaign. Geophysical Research Letters 25 (11), 1801–1804.

Tsai, H.F., Liu, J.Y., 1999. Ionospheric total electron content response to solar eclipses. Journal of Geophysical Research 104 (A6), 12657–12668.